Title
Mifepristone-inducible transgene expression in neural progenitor cells in vitro and in vivo

Journal
Gene Therapy, 23(5)

ISSN
0969-7128

Authors
Hjelm, BE
Grunseich, C
Gowing, G
et al.

Publication Date
2016-05-01

DOI
10.1038/gt.2016.13

Peer reviewed

HHS Public Access

Author manuscript

Gene Ther. Author manuscript; available in PMC 2016 August 08.

Published in final edited form as:

Gene Ther. 2016 May ; 23(5): 424–437. doi:10.1038/gt.2016.13.

Mifepristone-inducible transgene expression in neural progenitor cells *in vitro* and *in vivo*

BE Hjelm[1,6], **C Grunseich**[2,6], **G Gowing**[1], **P Avalos**[1], **J Tian**[1], **BC Shelley**[1], **M Mooney**[2], **K Narwani**[1], **Y Shi**[2], **CN Svendsen**[1], **JH Wolfe**[3,4], **KH Fischbeck**[2], and **TM Pierson**[1,5]

[1]Board of Governors Regenerative Medicine Institute, Cedars-Sinai Medical Center, Los Angeles, CA, USA

[2]Neurogenetics Branch, National Institute of Neurological Disorders and Stroke, NIH, Bethesda, MD, USA

[3]Departments of Pediatrics and Pathobiology, University of Pennsylvania, Philadelphia, PA, USA

[4]Stokes Research Institute, Children's Hospital of Philadelphia, PA, USA

[5]Department of Pediatrics and Neurology, Cedars-Sinai Medical Center, Los Angeles, CA, USA

Abstract

Numerous gene and cell therapy strategies are being developed for the treatment of neurodegenerative disorders. Many of these strategies use constitutive expression of therapeutic transgenic proteins, and although functional in animal models of disease, this method is less likely to provide adequate flexibility for delivering therapy to humans. Ligand-inducible gene expression systems may be more appropriate for these conditions, especially within the central nervous system (CNS). Mifepristone's ability to cross the blood–brain barrier makes it an especially attractive ligand for this purpose. We describe the production of a mifepristone-inducible vector system for regulated expression of transgenes within the CNS. Our inducible system used a lentivirus-based vector platform for the *ex vivo* production of mifepristone-inducible murine neural progenitor cells that express our transgenes of interest. These cells were processed through a series of selection steps to ensure that the cells exhibited appropriate transgene expression in a dose-dependent and temporally controlled manner with minimal background activity. Inducible cells were then transplanted into the brains of rodents, where they exhibited appropriate mifepristone-inducible expression. These studies detail a strategy for regulated expression in the CNS for use in the development of safe and efficient gene therapy for neurological disorders.

Correspondence: Dr TM Pierson, Board of Governors Regenerative Medicine Institute, Cedars-Sinai Medical Center, 8700 Beverly Boulevard, ASHP 8401, Los Angeles, CA 90048, USA. tyler.pierson@cshs.org.

[6]Co-first authors.

CONFLICT OF INTEREST

The authors declare no conflict of interest.

Supplementary Information accompanies this paper on Gene Therapy website (http://www.nature.com/gt)

INTRODUCTION

Numerous strategies using gene and cell therapy are being developed for the treatment of neurological disorders. To date, the majority of these strategies have used constitutive expression of therapeutic proteins in animal models of these disorders. Although this approach has shown promise in the laboratory, its future application in humans may be more limited because of the wider range of presentations associated with human disease and the variability of therapeutic responsiveness. For example, constitutive expression of therapeutic proteins at one concentration may benefit some patients, but produce unexpected side effects or a lack of benefit in others. Furthermore, non-regulated expression cannot be adjusted as individuals respond to therapy or have progression of their disease.[1,2] Because of these limitations, inducible gene expression systems may provide a more flexible and effective method to express therapeutic proteins within the central nervous system (CNS).

Several ligand-inducible systems have been developed for gene expression (e.g., the tetracycline, ecdysone, chemical inducer of dimerization and mifepristone (MFP) systems).[3] These systems use orally bioavailable ligands to activate engineered transcription factors for induction of transgene expression and have been successfully used *in vitro* and in animal models. Nevertheless, in order for them to be clinically applicable for human CNS disorders, these systems require several specific qualities. The inducible system should provide a wide range of dose-dependent transgene expression with negligible background activity. It should be composed mainly of human components to minimize immunogenicity, while also avoiding transgenic elements that have undesirable interactions with endogenous proteins or nucleic acids. Finally and most importantly, to be functional in the CNS, the activating ligand must be readily permeable to the blood–brain barrier.

The MFP-inducible gene expression system possesses many qualities that make it attractive for use in the CNS. This system uses a predominantly human-based synthetic nuclear hormone receptor (SWITCH) that binds and is activated by MFP to induce target gene expression from promoters possessing GAL4 upstream activating sequences (UAS).[4] This induction has very low basal activity and activates expression within hours of MFP exposure at concentrations 100–1000-fold less than those used in anti-progestin and anti-glucocorticoid therapies.[5–8] Of particular importance, MFP readily crosses the blood–brain barrier because of its amphiphilic steroid properties. Thus far, MFP-inducible expression has been used successfully in stable cell lines, viral delivery systems and zebrafish.[7–13] Inducible expression has also been observed in the CNS of transgenic animals.[14]

Of note, in the absence of selective pressure or intrinsic failsafe mechanisms, inducible systems will likely have some compromised fidelity. When fidelity is required, inducible systems should include strategies to cull cells constitutively expressing their transgenes in the absence of ligand, while also providing a selective advantage to cells exclusively activated by ligand exposure. These selection methods have faced some challenges and at this time cannot be safely used during direct viral infection of the CNS. Therefore, systems amenable to an *ex vivo* selection strategy before cell transplantation may provide the best means for effective and inducible CNS expression and therapy.

We report the development and characterization of murine neural progenitor cells (mNPCs) with MFP-inducible gene expression as a novel approach to CNS gene therapy. These inducible mNPCs were transduced *in vitro* with lentiviral vectors and were subjected to a selection strategy that ensured appropriate and flexible transgene expression. *In vitro* studies showed that the cells had MFP-inducible transgene expression that was dose-dependent, temporally controlled and capable of repeated activation and deactivation. *In vivo*, the system continued to have appropriate and inducible transgene expression following cell transplantation into rodent brain. Taken together, these results indicate that the MFP-inducible system is a strong candidate for use in the regulated delivery of therapeutic proteins to the CNS.

RESULTS

Vector design and strategy for the generation of MFP-inducible NPCs

The MFP system contains two basic components, a SWITCH locus and a TARGET locus, which were packaged into two separate self-inactivating lentiviral vectors[15] for *in vitro* delivery to mNPCs (Figure 1a). SWITCH vectors were used to express the chimeric nuclear receptor SWITCH, which consists of a truncated human progesterone receptor ligand-binding domain, the transcriptional-transactivation domain of human nuclear factor-κB-p65 and the DNA-binding domain of the yeast GAL4 transcription factor.[5] SWITCH binds MFP (but cannot bind progesterone) and subsequently activates transcription from promoters possessing Gal4 UAS elements.[4,5] SWITCH vectors had the SWITCH gene linked via an internal ribosome entry site (IRES)[16] to a selectable-marker gene (e.g., antibiotic-resistance genes or fluorophores) (Figure 1a). Auto-inducible expression of the SWITCH protein in mNPCs was driven by a promoter containing the second intron enhancer of the rat nestin gene[17] linked to UAS elements and a minimal thymidine kinase promoter (Figure 1). Concurrently, TARGET vectors were used for the inducible expression of TARGET transgenes in the presence of an MFP-activated SWITCH protein. These vectors possessed an MFP-responsive (UAS-containing) promoter upstream of two transgenes linked via an IRES (Figure 1a). These bicistronic vectors gave the system the capability to link the expression of a therapeutic gene-of-interest to a selectable-marker gene capable of both negative and positive selection (although the expression of the 3′ cistron is reduced with several IRES elements; see Materials and methods section). Of note, as these studies were proof-of-principle investigations to evaluate the fidelity of the system, we used a TARGET vector expressing two fluorophore proteins.

MFP-inducible mNPCs were generated in a stepwise manner. The initial steps consisted of the *in vitro* lentiviral infection of mNPCs with a SWITCH vector and subsequent selection of these putative SWITCH-expressing (SWITCH+) mNPCs using the selectable-marker gene in the second cistron of the vector. Once generated, these SWITCH+ mNPCs were infected with a TARGET vector and then underwent multiple rounds of negative and positive selection for enrichment of mNPCs that optimally expressed the system (Figure 1b). Negative selection involved the collection of NPCs not expressing TARGET transgenes in the absence of MFP, while positive selection involved the collection of NPCs expressing TARGET transgenes during MFP treatment (Figure 1b).

MFP-dependent auto-inducible expression of the SWITCH locus in NPCs

As most steroid receptors undergo activation-dependent degradation,[18,19] we ensured sufficient steady-state levels of cellular SWITCH protein were sufficient by using auto-inducible promoters in the SWITCH vectors. These vectors were similar in design, but used different selectable markers for selective enrichment of SWITCH+ cells. Vector 6A possessed the enhanced green fluorescent protein (eGFP)[20] gene for selection with fluorescence-activated cell sorting (FACS), while vector 6B contained a hygromycin-resistance ($Hygro^R$)[21] gene for antibiotic selection (Figure 2a). Murine NPCs derived from the subventricular zone (and enhanced for increased cell migration and survival by constitutive expression of EGFRvIII (see Materials and methods section for further details)) were infected *in vitro* with either vector 6A (6A-NPCs) or vector 6B (6B-NPCs) and subsequently selected. Western blots were used to evaluate the relative quantity of SWITCH protein in 6A- or 6B-NPCs in the presence or absence of MFP. MFP-treated 6A-mNPCs exhibited increased eGFP expression, indicating that the locus was inducible with MFP (Figure 2b); however, MFP-treated 6A- and 6B-NPCs also exhibited a paradoxical reduction in SWITCH protein levels (Figure 2b), indicating that the reduction in the SWITCH was likely the result of activation-dependent degradation similar to what occurs with other nuclear hormone receptors.[18,19] This phenomenon was evident in all subsequent evaluations.

MFP-dependent expression of the TARGET locus in NPCs and the effects of selection

TARGET vector 6D contains two transgenes, monomeric DsRed[22] and eGFP[20] (Figure 3a), and was used to infect 6B-NPCs (6B6D-NPCs). Several rounds of alternating negative and positive selection via FACS were used to obtain MFP-inducible 6B6D-NPCs (Figure 1b). Interestingly, the final round of selection, either negative or positive, was found to influence the subsequent expression characteristics of 6B6D-NPCs (Figures 3b and c). As such, we defined cells that were negatively selected in their final round of selection as undergoing a ‘stringent’ protocol, whereas 6B6D-NPCs treated with a final round of positive selection underwent a ‘relaxed’ protocol (Figure 3c). To define each cell’s transgene expression as either being ‘on’ or ‘off’, we established a threshold value of flow cytometry fluorescence intensity below which >99.9% of untreated ‘stringent’ 6B6D-NPCs resided. This threshold intensity value (log 10 = 3.8 (arbitrary units)) was equal for both DsRed and eGFP, and the percent of each cell population above this threshold was ascertained for each selection protocol in the presence or absence of MFP (Figures 3b and c). This threshold was also used later to evaluate the dose-dependent transgene expression of the 6B6D-NPCs (Figure 4g) and the effects of repeated transgene activation and inactivation (Figures 5f and h). In the absence of MFP, the 6B6D-NPC population subjected to the ‘stringent’ protocol had fewer cells with basal fluorescence activity or background for DsRed and eGFP (0.04% and 0.05%, respectively) than 6B6D-NPCs that underwent the ‘relaxed’ protocol (1.02% and 1.55%, respectively) (Figures 3b and c). These results indicate the ‘stringent’ protocol produces a cell population with somewhat less basal transgene activity in the absence of MFP, compared with those passed through the ‘relaxed’ protocol. While in the presence of MFP, 6B6D-NPCs subjected to the ‘relaxed’ protocol had a greater proportion of the cell population with inducible expression above our threshold for DsRed and eGFP (77.36% and 60.51%, respectively) than 6B6D-NPCs derived from the ‘stringent’ protocol (58.81% and 39.01%, respectively) (Figures 3b and c). Taken together, these data indicate that the

'relaxed' protocol generated a population of 6B6D-NPCs with higher MFP-inducible expression compared with those treated with the 'stringent' protocol, while basal expression was less in 6B6D-NPCs that underwent the 'stringent' protocol.

MFP dose-dependent expression of target transgenes *in vitro*

'Stringent' 6B6D-NPCs were exposed to a range of MFP concentrations *in vitro* (10^{-12}–10^{-8} M) and transgene expression was evaluated by western blot, flow cytometry and immunocytochemistry (Figure 4). MFP-treated mNPCs had healthy morphology and no obvious differences in their growth rates. Western blot analysis showed a dose-dependent increase in both DsRed (Figures 4a and c) and eGFP protein levels (Figures 4a and d). This increase in DsRed and eGFP expression was further supported by results with flow cytometry (Figures 4e–g) and immunocytochemistry (Figure 4h). Taken together, these data indicate that our selection strategy was highly efficient at deriving inducible cells *in vitro*.

TARGET transgene expression can be repeatedly activated and inactivated

We next investigated whether the MFP-inducible NPC system could be repeatedly activated and deactivated *in vitro*. Transgene expression was evaluated by western blot and flow cytometry using 'stringent' 6B6D-NPCs after they were subjected to repeated MFP exposure and withdrawal (Figure 5). To study transgene activation, cells were grown without MFP for 96 h (non-pretreated) and were then either treated with 10^{-8} M MFP or maintained without MFP for 48 or 96 h (Figures 5a–d). As expected, untreated mNPCs expressed only minimally detectable levels of fluorescent protein (lanes 1 and 4; Figures 5a, c and d), whereas MFP treatment increased the expression of DsRED and eGFP proteins during the period of MFP exposure (lanes 2 and 3; Figures 5a, c and d). Alternatively, to study transgene inactivation, cells were grown with 10^{-8} M MFP for 96 h (MFP-pretreated), and were then either treated with 10^{-8} M MFP or maintained without MFP for 48 or 96 h (Figures 5a–d). Continual MFP exposure resulted in persistent and high levels of detectable DsRed and eGFP proteins (lanes 6 and 7; Figures 5a, c and d), whereas MFP withdrawal resulted in a substantial reduction in these protein levels at 48 h postwithdrawal with further reduction observed after 96 h (lanes 5 and 8; Figures 5a, c and d) (please note: the half-life of eGFP is ~ 24 h, whereas DsRed is between 24 and 96 h (Corish and Tyler-Smith[20] and Verkhusha *et al.*,[22] personal communication; Clontech Laboratories, Mountain View, CA, USA).

To further understand MFP-dependent activation and deactivation, target gene expression was evaluated by flow cytometry over three cycles of MFP treatment and withdrawal (Figures 5e–h). Box-and-whisker plots were used to visualize the distribution of cells emitting DsRed (Figure 5e) and eGFP fluorescence (Figure 5g) within a single 21-day experiment. Both fluorophores showed robust increases in intensity after each 48 h MFP treatment (days 2, 9 and 16), followed by a reduction in fluorescence 48 h after MFP withdrawal (days 4, 11 and 18) and a subsequent decrease to approximately baseline levels 120 h after MFP withdrawal (days 7, 14 and 21) (Figures 5e and g). The percentage of cells above our previously defined intensity threshold was determined and used to calculate the mean and standard deviation between experiments (at each timepoint) and were also used for statistical analysis (Figures 5f and h). On day 0, the percent of 6B6D-NPCs with DsRed

and eGFP fluorescence above the threshold was minimal (ranging between 0.00–0.05% and 0.02–0.05%, respectively; Figure 5f). Exposure of MFP for 48 h (days 2, 9 and 16) consistently produced a robust increase in the percent of cells expressing both DsRed (69.85–84.68%; Figure 5f) and eGFP (28.37–44.30%; Figure 5h) and the mean percentages from each of these timepoints was significantly greater than day 0 ($P<0.01$ to <0.0001). Following 48 h of MFP withdrawal (days 4, 11 and 18), there was a consistent and marked decrease in the average percentage of cells expressing both DsRed (9.07–28.82%; Figure 5f) and eGFP (1.53–2.38%; Figure 5h); however, the majority of these timepoints were still significantly greater than day 0 ($P<0.05$ to <0.001). This indicates that, *in vitro*, 48 h of MFP withdrawal was insufficient for the population to completely return to baseline levels; however, 120 h of MFP withdrawal (days 7, 14 and 21) was sufficient for both DsRed (0.12–0.37%; Figure 5f) and eGFP (0.00–0.10%; Figure 5h).

In vivo MFP-inducible target transgene expression after cell transplantation

The *in vivo* activity of our system was evaluated by performing stereotactic injections of ‘relaxed’ 6B6D-NPCs into the brains of nude rats (‘relaxed’ cells were used because of their higher levels of inducible expression would provide us with a broader range of fluorescence detection for these initial animal studies).[1,23] Three days before cell transplantation, rats were subcutaneously implanted with timed-release pellets containing either placebo or MFP.[8] In each rat, non-pretreated 6B6D-NPCs were injected into the left hemisphere and MFP-pretreated 6B6D-NPCs were injected into the right hemisphere. This allowed evaluation of transgene activation in non-pretreated cells in MFP-treated animals as well as deactivation of MFP-pretreated cells in placebo-treated animals. The animals tolerated the procedure and MFP treatment well and were killed 10 days after cell transplantation. Histological inspection of the brains revealed that DsRed was easily observable without immunocytochemistry, whereas eGFP required anti-GFP immunocytochemistry for visualization (data not shown; there were also no overt tumors). Because of this pattern, we could use an anti-nestin primary antibody conjugated to a green fluorophore (results are shown as a white channel) to detect the grafts in all rats, as this coreacted with both infiltrating endogenous nestin-positive reactive cells around the graft[24,25] and (to a lesser extent) the transplanted 6B6D-NPCs. Conversely, an anti-DsRed antibody was used to further amplify and analyze the MFP-inducible transgene expression of our cells *in vivo* (Figures 6–8).

First, we performed qualitative analysis comparing placebo- and MFP-treated rats (Figure 6). Visual inspection showed no appreciable difference in DsRed fluorescence intensities between the left and right hemispheres of the same rat, indicating that transgene expression at that timepoint was because of the *in vivo* treatment rather than the *in vitro* pretreatment (Figures 6a–d). These results were further confirmed by CellProfiler[26] analysis of the fluorescent intensity ratio of the right/left hemispheres from several rats (Supplementary Figure S1). All sections analyzed showed approximately the same 1:1 ratio between the two hemispheres of the same rat. Visual comparisons between placebo- and MFP-treated rats revealed a marked increase in DsRed expression and fluorescence with MFP treatment, which was even more obvious with DsRed immunostaining (Figure 6). Of note, each transplant site had a collection of cells in the graft core that emitted a low level of red

fluorescence regardless of treatment with placebo or MFP; this signal was observed in cells with a spherical morphology and likely represents dead cells within the core of the transplant site (Figures 6e and g)[27] In contrast, only MFP-treated rats had NPCs with a much higher level of red fluorescence intensity and also the spindle-shaped morphology of viable NPCs (Figures 6f and h).

We next performed ImageJ[28] analysis comparing brain grafts of placebo- and MFP-treated rats (Figure 7). Images were selected based on section and image quality irrespective of hemisphere, as this variable was previously determined to have no noticeable effect (Supplementary Figure S1). Grayscale images of nestin-positive cells indicated each section had similar levels of nestin immunoreactivity (Figure 7a), which was also evident with thermal LUT transformation (Figure 7a). Plots of gray values across the nestin grayscale image showed similar levels of nestin signal intensities between the two groups (Figure 7c); similarly, surface plots from the thermal LUT images showed similar staining patterns and intensities (Figure 7d). These results support the conclusion that similar graft sections or images were chosen for analysis between groups. Grayscale images of DsRed-positive areas demonstrated an obvious difference in transgene expression between the placebo- and MFP-treated rats, which was further supported after image transformation (Figure 7b). Plots of gray values across the DsRed grayscale image revealed increased fluorescence in the MFP-treated rats in comparison with the values in the placebo group; this difference was also evident in surface plots from the thermal LUT images (Figure 7f).

Finally, CellProfiler[26] was used to quantitate the number of DsRed-positive mNPCs in regions with a large cluster of endogenous nestin-positive reactive cells[24,25] (Supplementary Figure S2). By quantifying the nestin and DsRed signals adjacent to the transplant site, this analysis allowed for single-cell identification as well as eliminating potential concerns associated with autofluorescent material within the graft cores.[27] Nestin immunoreactivity was not significantly different between treatment groups with regard to: (1) total image area, (2) the number of nestin-positive cells or (3) signal intensity (Figures 8a, b and f). In contrast, there were significantly more DsRed-positive cells identified in MFP-treated rats than the placebo group (Figures 8c–e). Similarly, DsRed signal intensity identified through CellProfiler was also significantly higher in MFP-treated rats (of note: this amount does not reflect ‘fold induction’ as this technology is not adequately sensitive to precisely measure protein expression (i.e., it is not as sensitive as FACS or western blot for this value)) (Figure 8g). Overall, both automated and visual examination of the graft regions, as well as quantitative analysis of migrating mNPCs, support our conclusion that an NPC-based MFP-inducible system can effectively regulate gene expression in the CNS.

DISCUSSION

We have modified and adapted the MFP-inducible system and shown its successful function in mNPCs, thereby generating a promising *ex vivo* system for use within the CNS. Correlating with previously published results,[5] our inducible mNPCs were responsive to MFP over several orders of magnitude, with the broadest range of expression observed across a 100-fold dosage range (10^{-11}–10^{-9} M; a range not associated with antagonism of the progesterone or glucocorticoid receptors). Importantly, we also found that the system

was capable of repeated activation and deactivation to permit flexible gene delivery. Experiments also quantifiably indicated that an autoinduction loop within the SWITCH locus may be the best means of expressing the nuclear receptor because of its use-dependent degradation. This also enabled us to express the nuclear receptor at relatively low baseline levels (reducing chances of any potential toxicity when idle) and then increase SWITCH expression when it was needed to activate the TARGET locus. Interestingly, our results indicate that this degradation was also dose-dependent and temporally controlled. These studies indicated that the steady-state SWITCH protein levels had the potential to drop precipitously during activation, with autoinduction providing an adequate increase in expression for stable steady-state levels of SWITCH protein to be available in the presence of MFP.

Our system contained a bicistronic TARGET vector designed for coexpression of a therapeutically relevant gene-of-interest along with a selectable-marker gene. For these initial proof-of-principle studies, we used a TARGET vector coexpressing monomeric DsRed[22] and eGFP,[20] which were used for negative and positive selection steps, as well as the evaluation of TARGET transgene expression *in vitro* and *in vivo*. The results indicated that these selection strategies markedly enhanced the fidelity of the system; nevertheless, we found that the final selection criteria still had an influence on the expression dynamics of these polyclonal NPC populations. Although FACS was used for both selection steps in the current strategy, future strategies to increase fidelity could include TARGET vectors with selectable markers such as thymidine kinase[29] (for negative selection) and/or other antibiotic-resistance genes[21] (for positive selection). At this time, none of these selection methods can be efficiently or safely used with direct viral infection of endogenous neural cells within the CNS. As such, our cell-based gene therapy approach, amenable to *ex vivo* selection steps and extensive characterization before CNS transplantation, may provide the best means to safely and efficiently induce therapeutic gene expression in the brain. Of course, when a treatment requires less rigorous fidelity, this system may be altered to accommodate those needs. These investigations provided basic proof-of-principle with fluorescent markers as an important first step towards future studies that may include vectors expressing therapeutic transgenes such as neurotrophic factors and other secretory proteins with neuroprotective effects.[1,23,30–32]

Neural progenitor cells have many qualities that make them attractive vehicles for use within the CNS. Substantial evidence indicates that NPCs transplanted into animal models of disease are able to survive, differentiate and integrate into the damaged parenchyma.[33–41] Furthermore, NPCs expressing therapeutic proteins have been successfully transplanted into animal models of neurodegenerative disease with amelioration of symptoms and pathology.[30–35] By incorporating a nestin-enhancer element into the SWITCH vectors, we were better able to optimize their use in our mNPCs.[17] Although this facet of the system is not an obligatory element for the expression of the SWITCH vector in NPCs, it enabled us to enhance the basal expression of the SWITCH protein in NPCs compared with other differentiated neural cells (Supplementary Figure S3). Murine NPCs were used for these initial studies because they are easier to manipulate and expand, and EGFRvIII expression was added to enhanced survival of transplanted NPCs in unlesioned brains; nonetheless, human NPCs (that do not need to be engineered with EGFRvIII) are an obvious clinically

relevant cell type for future studies. While the availability and diversity of tissue-derived human NPC lines are limited, induced pluripotent stem cells and induced neural progenitor cells[41–46] may provide additional options for introducing the system into patient-specific cells for personalized therapy.

Finally, we demonstrated that this MFP-inducible system functions both *in vitro* and *in vivo* within the brain. The induction of expression within the brain is particularly important for potential CNS gene therapy. Future studies of this system's capacity to deliver inducible therapy may include *in vivo* studies in animal models of neurodegenerative disease and direct experimental comparisons with other inducible methods (e.g., tetracycline). Additional *in vivo* variables will need to be systematically evaluated to further elucidate the MFP-system's specific clinical requirements, including MFP dosage, exposure time, repeated exposure and withdrawal, and the stage of disease, as well as any specific issues regarding the system's use in clinically applicable cells lines (e.g., the propensity for these cell lines to undergo differentiation and tumorigenicity and the resultant effects on this system). Overall, our results confirm that the MFP system is a valuable tool for CNS therapeutic delivery and complement ongoing strategies to use NPCs for the CNS delivery of therapeutic proteins for neurodegenerative disorders.

MATERIALS AND METHODS

Lentiviral vectors for MFP-inducible expression

The Lentilox 3.7 (LL3.7) lentiviral backbone (gift from Tyler Jacks Lab, Cambridge, MA, USA) was used to produce self-inactivating vectors containing the MFP-inducible system.[47] The GeneSwitch system was purchased from Invitrogen (now Life Technologies, Grand Island, NY, USA), and both the regulatory plasmid (pSwitch) and inducible expression plasmid (pGene/V5-His) were used and genetically modified as part of our various SWITCH and TARGET vectors, respectively.[5] Briefly, our SWITCH vectors (6A and 6B) were modified to contain the second intron enhancer of the rat nestin gene[17] (from plasmid pTYNestinHSP68-eGFP; gift from Steven Goldman Lab, Rochester, NY, USA); this element was introduced upstream of six copies of the UAS (from GeneSwitch plasmid pGene/V5-His) linked to the minimal herpes simplex virus thymidine kinase promoter and SWITCH protein coding sequence (both from GeneSwitch plasmid pSwitch). The SWITCH protein and a selectable-marker gene were transcriptionally linked via a poliovirus internal ribosomal entry site (IRES) element[16] (from plasmid pHPIS; gift from Hansjorg Hauser Lab, Braunschweig, Germany). Vector 6A possessed the eGFP gene in its 3′ cistron (from plasmid pLL3.7; gift from the Tyler Jacks lab), whereas Vector 6B contained a hygromycin-resistance gene (from GeneSwitch plasmid pSWITCH) in this position. TARGET vector 6D was generated to contain similar UAS and minimal promoter elements as the SWITCH vectors (UASx4 and minimal thymidine kinase; both from GeneSwitch plasmid pSwitch); however, downstream of the MFP-inducible promoter, the locus was engineered to contain the coding sequences of two fluorophores, monomeric DsRed[22] in the 5′ cistron (from plasmid pDsRedMonomer-C1; Clontech) and eGFP[20] in the 3′ cistron (from plasmid pLL3.7) linked via the same poliovirus IRES (note: cDNAs translated with a poliovirus IRES are known to be produced at ~ 20–30% of those translated by a 5′ cap-mediated

mechanism). All of the generated vector plasmids were evaluated by transient transfection in HEK293T cells before production of the virus to assay expression of individual transgenes (data not shown). Lentivirus was produced using the ViraPower Lentiviral Packaging Mix (Life Technologies) according to the manufacturer's instructions. Media containing lentiviral particles were collected, clarified and concentrated by centrifugation with Amicon 100 kDa filters (Millipore, Billerica, MA, USA). Viral titers were determined with the Global UltraRapid Lentiviral Global Titer Kit (System Biosciences, Mountain View, CA, USA) as per the manufacturer's instructions; quantitative PCR was performed on the Applied Biosystems 7900HT Fast Real-Time PCR System (Life Technologies).

Murine NPC culture and lentiviral infections

All animal work was approved by the International Animal Care and Use Committee (IACUC) of the Children's Hospital of Philadelphia and Cedars-Sinai. All tissue culture flasks were precoated with 10 μg ml^{-1} poly-D-lysine (Sigma-Aldrich, St Louis, MO, USA) overnight at room temperature and rinsed two times with phosphate-buffered saline (PBS) before use. Murine primary neural progenitor cell lines were generated as described previously (see Supplementary Methods for further details)[48] and maintained in 'mNPC-media' consisting of Dulbecco's modified Eagle's media (Life Technologies) containing 1% fetal bovine serum, 1% N2 supplement, 2 mM L-glutamine, 1% penicillin/streptomycin (Life Technologies) and 20 ng ml^{-1} basic fibroblast growth factor (Promega, Madison, WI, USA) in a 37 °C and 5% CO_2 incubator. mNPCs were infected with lentiviral vector pTY-EF-EGFRvIII for constitutive expression of the human EGFRvIII variant of the epidermal growth factor receptor. This variant has been shown to enhance cell survival and motility after transplantation into the unlesioned murine CNS.[49] Vector pTY-EF-EGFRvIII was generated with the pTY-linker plasmid (gift from the NIH AIDS Reagent Program, Germantown, MD, USA) using the human EF1α promoter to express the EGFRvIII (gift from the Webster Cavenee lab (San Diego, CA, USA) and the Ludwig Institute for Cancer Research, San Diego, CA, USA); virus was generated as described previously. Cells were expanded after infection and live cells were stained with a mouse anti-human EGFR antibody (1:500, Ab-10, ab231; Labvision, Kalamazoo, MI, USA) and a goat anti-mouse secondary antibody (1:500, Alexa Fluor 488, A-11001; Life Technologies). Positively stained cells were sorted and collected by FACS using a FACSVantage SE cell sorter (BD Biosciences, San Jose, CA, USA) (data not shown). EGFRvIII+ mNPCs were used in all experiments; unfortunately, the mouse anti-human EGFR antibody used for FACS did not robustly stain transplanted cells *in vivo* and could not be used to localize transplant grafts. This murine cell line was not authenticated short tandem repeat analysis, karyotyping or tested for mycoplasma contamination before experimentation.

Lentiviral infections were all carried out in 24-well plates coated with 10 μg ml^{-1} poly-D-lysine (Sigma-Aldrich). Cells were plated at ~ 5×10^4 cells per well one day before lentiviral transductions. Lentivirus stock was pipetted into NPC media (without fetal bovine serum and antibiotic) to add to cells at a multiplicity of infection of 5–15. Cells were incubated with virus for up to 24 h and fresh media were exchanged before cell line expansion. mNPCs were first infected with one of our SWITCH vectors (6A or 6B); these cells were then expanded and selected by FACS or resistance (see below). After selection,

SWITCH+ mNPCs (6A-NPCs or 6B-NPCs) were expanded and tested for SWITCH expression (see below). 6B-NPCs were then reinfected with our TARGET vector (6D) and a series of fluorophore-based FACS selections were carried out to isolate MFP-inducible NPCs (see below).

Fluorophore and antibiotic-based selection

mNPCs infected with vector 6A (6A-NPCs) were treated with 10^{-8} M MFP (Life Technologies) for 3–4 days to amplify eGFP expression before FACS. Cells were incubated in 2 ml of 0.05% trypsin (Life Technologies) in PBS for 15–20 min at 37 °C and the reaction was stopped by the addition of 1 ml of fetal bovine serum (HyClone; GE Healthcare, Logan, UT, USA). 6A-NPCs were then resuspended in 2 ml of 0.125 mg ml^{-1} of DNase I (Sigma-Aldrich) in PBS for 10 min and eGFP+ cells were collected by FACS using the FACSCalibur system and CellQuest software (BD Biosciences). All cells were collected in a non-clonal manner for expansion and so represent polyclonal cell lines. These non-clonal cells were then expanded to generate protein lysates for western blot analysis of SWITCH protein and eGFP expression. Cell stocks were frozen by cryopreservation in 10% dimethyl sulfoxide (Sigma-Aldrich).

mNPCs infected with vector 6B (6B-NPCs) were treated with 10^{-8} M MFP for 3–4 days for transgene expression before selection with hygromycin (150–400 μg ml^{-1}; Life Technologies) over 1–2 weeks. Surviving 6B-NPCs were continually grown in the presence of 100 μg ml^{-1} hygromycin for all subsequent experiments. Hygromycin-resistant 6B-NPCs were then expanded polyclonally and used to generate protein lysates for western blot analysis of Switch protein expression. These cells were also used for differentiation studies (Supplementary Figure S1). Cell stocks were frozen by cryopreservation in 10% dimethyl sulfoxide.

6B-NPCs were subsequently infected with vector 6D (6B6D-NPCs) and underwent a series of positive and negative FACS selection steps to obtain MFP-inducible cells with low basal activity. These steps had 6B6D-NPCs first processed through a negative selection step, whereby non-MFP-treated 6B6D-NPCs underwent FACS selection and only 6B6D-NPCs that were negative for fluorescence were collected; this negative selection was performed to remove cells with any constitutively active transgene expression (i.e., likely due to factors related to their vector integration sites). Cells then underwent a positive selection step, whereby cells were then treated with 10^{-8} M MFP for 3–4 days, and cells with positive DsRed/eGFP fluorescence were collected by FACS. FACS was performed using the FACSCalibur system and CellQuest software (BD Biosciences). These alternating negative and positive selection steps were then repeated until the cells had gone through six sorts. A seventh and final FACS sort was performed that was either negative (‘stringent’ protocol) or positive (‘relaxed’ protocol) and the resultant cell populations were analyzed for DsRed and eGFP fluorescence by flow cytometry using the BD LSRFortessa cell analyzer (BD Biosciences) to determine if these protocols affected baseline or inducible expression. ‘Stringent’ 6B6D-NPCs were used for all subsequent *in vitro* experiments, whereas ‘relaxed’ selected 6B6D-NPCs were used for *in vivo* studies (to have some minimal baseline expression of fluorophores to better localize placebo-treated 6B6D-NPCs *in vivo*).

Western blot analysis

mNPCs were lysed with ice-cold RIPA buffer (50 mM Tris (pH 8.0), 150 mM NaCl, 1% NP-40, 0.5% sodium deoxycholate, 0.1% sodium dodecyl sulfate) supplemented with Complete Protease Inhibitor Cocktail Tablets (Roche, Mannheim, Germany). The lysates were centrifuged at 20 000 *g* for 20 min at 4 °C. Protein samples were quantified by Bradford assay (Thermo Fisher Scientific, Rockford, IL, USA) and equals amounts were denatured for 5 min at 95 °C in 4× sodium dodecyl sulfate sample buffer (0.25 M Tris-HCl (pH 6.8), 4% (w v^{-1}) sodium dodecyl sulfate, 10% (v v^{-1}) β-mercaptoethanol, 20% (v v^{-1}) glycerol, 20 mg ml^{-1} bromphenol blue) (Life Technologies), and separated by sodium dodecyl sulfate-polyacrylamide gel electrophoresis. Protein was then electrotransferred onto polyvinylidene difluoride membranes (Life Technologies). Membranes were subsequently blocked with 5% skim milk powder in TBS-T (Tris-buffered saline+0.1% Triton X-100) for 1h at room temperature and then incubated with primary antibody solution in 5% milk/TBS-T solution overnight at 4 °C. The membranes were rinsed with TBS-T and were then incubated with peroxidase-conjugated goat anti-rabbit (or goat anti-mouse) secondary antibodies (Jackson ImmunoResearch Laboratories, West Grove, PA, USA) for 1 h at room temperature. The proteins were detected with Western Lighting Plus ECL chemiluminescence HRP substrate (Perkin-Elmer, Waltham, MA, USA). For additional relabeling, the membrane was stripped with ReBlot Plus Mild Antibody Stripping Solution (Millipore, Billerica, MA, USA) according to the manufacturer's instructions, and was then reincubated with primary antibody after blocking. Primary antibodies used (and their dilutions) were against nuclear factor-κB (1:1000; A632536; Abcam, Cambridge, MA, USA), DsRed (1:1000; 632496; Clontech Laboratories), eGFP (1:1000; A11122; Life Technologies) and β-actin (1:3000; A5316; Sigma-Aldrich). Results were similar with two to four repetitive cohorts. Relative protein quantifications were determined with ImageJ software (Bethesda, MD, USA) for each individual western blot.

Flow cytometry analysis

6B6D-NPCs exhibited MFP-inducible expression of the DsRed and eGFP transgenic fluorophores. Flow cytometry analysis was performed on the NPC populations to evaluate the relative fluorescence intensities (arbitrary units) of these fluorophores in each individual cell and across the cell populations. Briefly, NPCs were incubated in 2 ml of 0.05% trypsin (Life Technologies) in PBS for 15–20 min at 37 °C and the reaction was stopped by the addition of 1 ml of murine neural progenitor cell (HyClone; GE Healthcare). Cells were then centrifuged and resuspended in 2 ml of 0.125 mg ml^{-1} of DNase I (Sigma-Aldrich) in PBS and were incubated on ice for 10 min. Flow cytometry was performed with a BD LSRFortessa cell analyzer (BD Biosciences) using 10 000 cells as input for all experiments (before gating), and the FITC and PE filters were used to evaluate the eGFP and DsRed levels, respectively. FCS files were exported and converted to text files using flowCore[50] software (Heidelberg, Germany) (part of the Bioconductor[51] R package) in RStudio.[52] All samples were gated according to the following parameters: (1) 50 000<FSC. A<250 000; (2) SSC.A<250 000; (3) SSC.W<138 895; (4) SSC.A/FSC.A<1.5; (5) FSC.W/FSC.H<2.427934.

Scatter plots of NPCs under our 'relaxed' and 'stringent' selection schemes were generated in RStudio.[52] All plots display the relative fluorescence intensity (arbitrary units) of eGFP (x axis) versus DsRed (y axis) for each cell on a log 10 scale. Evaluation of our 'stringent' selection strategy by western blot analysis and immunofluorescence indicated minimal or undetectable background levels of transgene (fluorophore) expression in the absence of MFP. As such, we used these guidelines to set a minimal fluorescence threshold value for a cell to be defined as being 'on'. This value was defined as the relative intensity below which 99.9% of untreated 'stringent' 6B6D-NPCs resided. This value was equal for both eGFP and DsRed (log 10 scale = 3.8 (arbitrary units)) and was used to evaluate the percent of the cell population that was above this value for each fluorophore (independently). We also used these metrics to evaluate the percent of the cell populations with positive fluorescence in several experiments. Last, we also graphed the distribution of the cell populations for both fluorophores using box-and-whisker plots for several flow cytometry experiments. Box-and-whisker plots were created in RStudio.[52] Briefly, box borders display the first and third quartile, or the 25th and 75th percentile, respectively, whereas the midline represents the second quartile or 50th percentile. Box whiskers were defined according to the default settings (i.e., the interquartile range $\div\sqrt{n} \times 1.58$); data points outside of this range (i.e., outliers) are shown as points on the graph.

Immunocytochemistry

mNPCs were evaluated for DsRed and eGFP fluorescence by immunocytochemistry without MFP or following exposure to a range of MFP concentrations (10^{-12}–10^{-8} M). A total of 5×10^4 mNPCs were plated onto poly-D-lysine-coated glass coverslips (22 mm^2) and grown in mNPC-media with or without MFP for 3 days. Coverslips were then rinsed with PBS and fixed with 4% paraformaldehyde (Electron Microscopy Sciences, Hatfield, PA, USA) for 15 min at room temperature. Coverslips were then rinsed and stored in PBS. DsRed and eGFP fluorescence signals were antibody-amplified independently as both primary antibodies used were both generated from rabbit. Fixed coverslip cultures were permeabilized with 0.15% Triton in PBS for 10 min at room temperature on an orbital shaker, then rinsed and blocked in a solution of 5% bovine serum albumin (BSA) (Sigma-Aldrich) in PBS for 30 min at room temperature. The blocking solution was then replaced with primary antibodies against eGFP (1:1000; A11122; Life Technologies) and DsRed (1:500; 632496; Clontech Laboratories) in a solution of 2.5% BSA/PBS-T (PBS+0.1% Tween-20) and the coverslips were allowed to incubate overnight at 4 °C on an orbital shaker. Following incubation with primary antibody, the coverslips were rinsed 3× for 10 min with PBS-T and were blocked again, followed by incubation in AlexaFluor488 goat anti-rabbit (1:1000, A11034; Molecular Probes/Invitrogen, Eugene, OR, USA) and AlexaFluor594 goat anti-rabbit (1:1000, A11037; Molecular Probes/Invitrogen) secondary antibodies in a solution of 2.5% BSA/PBS-T for 2 h at room temperature in the dark on an orbital shaker. Following incubation with secondary antibody, the coverslips were rinsed 3× for 10 min with PBS-T, and nuclei were counterstained using DAPI (4′,6-diamidino-2-phenylin-dole) according to the manufacturer's instructions (Sigma-Aldrich). Coverslips were mounted onto slides using Fluoromount-G mounting media (Southern Biotech, Birmingham, AL, USA).

Animal studies

Animals—Animal studies were performed to evaluate the *in vivo* activity of our MFP-inducible NPCs. This study was approved by the International Animal Care and Use Committee (IACUC) of Cedars-Sinai Medical Center.

Approximately 2-month-old male nude rats (Crl:NIH-Foxn1^{rnu}; Charles River Laboratories, San Diego, CA, USA) were acclimated for several weeks at our facility before procedures. Six rats (divided into equal groups of placebo- or MFP-treated) were used for these studies, immunohistochemistry and imaging analysis (see below). Group sample size and analysis of which fluorophore (i.e., eGFP or DsREd) and which cell protocol (i.e., 'stringent' or 'relaxed') would result in the greatest effect size between groups was determined by comparing the cell proportions in the ON (+MFP) and OFF (− MFP) conditions *in vitro* (Figures 3b and c). It was determined that evaluating the DsRed signal from cells derived from the 'relaxed' protocol would result in the greatest effect size, with the smallest group size ($N = 3$) needed to achieve Power of 0.8 with a predicted Type 1 error rate (α) of 0.05. Similar analyses demonstrated 6–13 animals per group would be required to detect an effect with the eGFP signal or with cells derived from the 'stringent' protocol; as such, we chose to evaluate the inducible expression of DsRed *in vivo* from cells derived form the 'relaxed' protocol as this limited the number of live animals required for this proof-of-principle study. Twenty-one-day timed-release pellets containing either placebo or 31 mg MFP (Innovative Research of America, Sarasota, FL, USA) were used to evaluate the *in vivo* activity of our MFP-inducible NPCs.

Surgical preps—For both pellet implantations and cell transplantation surgeries, rats were anesthetized by continuous inhalation of isofluorane and were administered subcutaneous injections of carprofen (5 mg kg^{-1}) and buprenorphine (0.05 mg kg^{-1}) for postoperative analgesia. Rats were shaved on the neck and head regions for the pellet implantations and cell transplantations, respectively.

Pellet implantations—A single pellet (MFP or placebo) was placed under the animal's skin by subcutaneous implantation on the lateral side of the neck between the ear and the shoulder according to the pellet manufacturer's instructions. The site was then closed with a single surgical staple. Randomization of animals for group assignments was not used, animals were assigned to groups in pairs so that rats cohoused would receive the same treatment; this setup was important to diminish the chance that MFP exposure could occur via fecal–oral exposure. Three days after the pellet implantations, the rats were prepped for cell transplantation surgeries.

Cell preparation—6B6D-NPCs derived from the 'relaxed' protocol were split into two groups: (1) 'Non-Pretreated' cells were grown for at least 1 week without MFP, and (2) 'MFP-Pretreated' cells were grown for at least 1 week in the presence of 10^{-8} M MFP. Cells were trypsinized by the addition of 5 ml TrypLE solution (Invitrogen, and so on) and were allowed to incubate for 15 min at 37 °C. Cells were resuspended in basal media, pelleted by centrifugation (200 *g* for 5 min) and were treated with 2 ml of 0.125 mg ml^{-1} of DNase I (Sigma-Aldrich) in PBS for 10 min. Cells were again pelleted by centrifugation,

resuspended in basal media and were pushed through a 40 μm filter by pipette. Viable cells were counted using a hemocytometer and Trypan Blue stain, and cells were pelleted again by centrifugation and resuspended in Hibernate-E media (Gibco, Life Technologies, site; Carlsbad, CA, USA) at a final concentration of 200 000 cells per μl. Cells were kept on ice before and during cell transplantation surgeries.

Cell transplantation surgeries—Animals were prepped for surgery as described previously. Although under continuous anesthesia, rats were secured for stereotactical injections. Each rat received bilateral transplants into the striatum/brain,[1,23] one at site AP − 0.6, ML +2.6, DV − 5.0 and another at site AP − 0.6, ML − 2.6, DV − 5.0, for a total of two injections per rat (i.e., one per hemisphere). A 10 μl Hamiton syringe with beveled 27G needle was lowered 5.5 mm from dura, and retracted 0.5 mm to create a 'pocket' for the cells. Two microliter of cells (400 000 cells total) were injected over 2 min, and the needle was retracted after an additional 2 min wait period. This procedure was then repeated in the contralateral hemisphere. 'Non-Pretreated' 6B6D-NPCs were injected into the left hemisphere of each rat, whereas 'MFP-Pretreated' 6B6D-NPCs were injected into the right hemisphere of each rat. Surgical site was closed by discontinuous suturing with Monocryl 4-0 absorbable sutures, and animals were monitored postoperatively and for the duration of the study for side effects. The presence of side effects and/or encapsulation of the MFP pellet (which could affect drug absorption) was used as the exclusion criteria for this study; however, no animals were observed to have side effects or encapsulation of the MFP pellet; therefore, no animals were subsequently excluded.

Terminal sacrifices—Ten days after cell transplantation surgeries, rats were humanely killed by cardiac perfusion following intraperitoneal injections of anesthesia (100 mg kg^{-1} ketamine and 10 mg kg^{-1} xylzine). Animals were perfused with PBS followed by 4% paraformaldehyde. Brains were then manually removed and were fixed in 4% paraformaldehyde for an additional 24 h, followed by storage in a 20% sucrose solution at 4 °C. Blinding was not used during group assignment and/or assessment of brains by immunohistochemistry.

Immunohistochemistry

Brains were sectioned at 30 μm using a modified Leica SM 2010R microtome, and sections were stored in 30% sucrose, 30% ethylene glycol, in 0.1 M phosphate buffer) at − 20 °C before immunohistochemistry. All staining procedures were performed while sections were in liquid suspension, before mounting on coverslips/slides. All permeabilization and antibody staining steps were performed in 48-well plates and washing and blocking steps were performed in 12-well plates.

Brain sections were rinsed 3× with Dulbecco's PBS, then permeablized with 0.15% Triton X-100 in PBS (PBS-T) for 30 min at 37 °C and finally blocked with 5% BSA in Dulbecco's PBS for 30 min at room temperature. Sections were then incubated with an anti-nestin antibody (1:100, MAB353; Chemicon Millipore, Billerica, MA, USA) and an anti-DsRed (1:500, 632496; Clontech) in 2.5% BSA/PBS-T for 30 min at 37 °C and then overnight at 4 °C on an orbital shaker. Following this incubation, the sections were rinsed 3× for 10 min

with PBS-T and were blocked again as described previously, followed by incubation with AlexaFluor488 goat anti-mouse IgG (1:1000, A-11001; Molecular Probes/Invitrogen) and AlexaFluor594 goat anti-rabbit (1:1000, A11037; Molecular Probes/Invitrogen) secondary antibodies in 2.5% BSA/PBS-T for 2 h at room temperature on an orbital shaker in the dark. The sections were rinsed 3× for 10 min with PBS-T followed by nuclei counterstaining with DAPI according to the manufacturer's instructions (Sigma-Aldrich). Sections were mounted onto coverslips using Fluoromount-G mounting media (Southern Biotech, Birmingham, AL, USA) for future microscopy.

Imaging analysis

Imaging analysis was performed on immunohistochemistry-stained brain sections to evaluate the DsRed fluorescence (i.e., transgene expression) between several rats receiving MFP versus placebo (Figures 6–8). First, we performed qualitative analysis of sections with fluorescence microscopy after anti-DsRed and anti-Nestin immunostaining of rats that received placebo versus MFP pellets (Figure 6). Visual inspection suggested there was no difference in DsRed fluorescence intensities between the left and right hemispheres of the same rat, suggesting that the *in vitro* pretreatment did not have a lasting effect on transgene expression. These results were further confirmed by CellProfiler[26] analysis of the fluorescent intensity ratio of the right/left hemispheres from several rats, and all sections analyzed resulted in approximately the same 1:1 ratio between the two hemispheres (Supplementary Data S1). However, visual inspection did show a prominent difference in DsRed fluorescence between the groups, where the rat receiving MFP showed much greater transgene expression than the rat that received placebo. These results were additionally confirmed by analyses in ImageJ, CellProfiler, and statistics from the resulting cell counts (Figures 7 and 8).

ImageJ[28] analyses were then performed on the brain grafts of two rats that received placebo versus two that had received MFP pellet treatment (Figure 7). Images were selected based on section and image quality, irrespective of hemisphere since this variable was previously determined to have no noticeable effect. The four (total) images were merged into a single 720 pixel (W) × 540 pixel (H) image, where grafts from rats receiving the placebo were aligned vertically on the left half of the image and grafts from rats receiving MFP were aligned vertically on the right half of the image. The image channels (red = DsRed and white = Nestin) were split so that the respective stains could be analyzed independently, and the resulting images were converted to 32-bit grayscale images. These grayscale images were then analyzed for the average fluorescence intensity across the x axis, and as such, the relative intensity of the left versus right side of the image could be compared and display any difference between the treatment groups. This analysis was performed for the Nestin (white channel) image,[24,25] in order to confirm the same graft region was selected for both groups, as well as the DsRed (red channel) image, to evaluate the relative level of transgene expression. In addition, grayscale images were transformed into a spectral color scale using the Thermal LUT reference file; a surface plot of this Thermal LUT image was also generated in ImageJ (Figure 7). These multiple imaging analysis schemes all supported the conclusions that similar graft regions were chosen for analysis (i.e., Nestin images/plots were similar between right and left side of image), but that the MFP group had greater

transgene expression than the placebo group (i.e., DsRed images/plots displayed greater intensities on right side of image versus left).

Last, we performed CellProfiler[26] analysis on images that displayed Nestin-reactivity adjacent to the location of, but not including, the transplant site. This analysis used the presence of endogenous Nestin-positive reactive cells adjacent to the grafts,[24,25] but did not include the possible confounding influence of autofluorescent material (i.e., dead cells) at the transplant sites themselves.[27] DsRed-positive cells that had migrated to this region were counted and analyzed. Images from rats that received the MFP pellets versus placebo (N = 3) were used and the following measurements were quantified: (1) the percent of the image area occupied by Nestin-positive staining; (2) the number of Nestin-positive objects (cells) in the respective image; (3) the mean image intensity from the Nestin-immunoreactive image channel; (4) the number of DsRed-positive cells in the respective image; and (5) the mean intensity of DsRed-positive cells. To ensure DsRed evaluations were performed between similar sections/images, the number of DsRed cells in each image was normalized to both the percent of the image area occupied by Nestin-positive staining and to the number of Nestin-positive objects (cells) counted in the respective image. Standard deviation error bars displayed on the graphs represent the variance between the three rats or replicates evaluated (Figure 8). Statistical tests were performed between the MFP and placebo groups on all measurements described, both pre- and postnormalization (Figure 8).

Statistical analysis

All statistical tests were carried out using RStudio.[52] For all statistical analyses, normality was tested by visual inspection of normal probability plots (P–P) and analysis by the Shapiro–Wilk test of normality. In addition, homogeneity of variances was tested using an F-test for variance. For all subsequent tests, statistical significance is displayed as follows: ^P<0.05; *P<0.01; **P<0.001; ***P<0.0001.

Statistical analysis was performed on flow cytometry data from our activation and deactivation time-series experiment (Figures 5f and h). Analysis of the population percentages that were above our threshold for positive expression was performed using independent replicates (N = 3) with variance displayed as standard deviation error bars. Statistical comparisons were performed between the day 0 timepoint versus all other timepoints to determine how repeated MFP exposure and withdrawal affected the population's fluorescence (i.e., transgene expression). Testing of parametric assumptions demonstrated these groups followed a normal distribution, but had a significant difference in variance (data not shown); as such, Welch's t-tests were performed on the population percentages to test for statistical significance.

Statistical analysis was performed on cell counting data obtained from CellProfiler[26] (Figure 8). Testing of parametric assumptions demonstrated these groups followed a normal distribution and had equivalent variances between all comparisons (data not shown); as such, parametric t-tests were performed on all measurements to test for statistical significance between MFP and placebo groups.

Supplementary Material

Refer to Web version on PubMed Central for supplementary material.

Acknowledgments

We are grateful to Trena Clarke (University of Pennsylvania), Kelli DeJohn, Jacalyn McHugh, Roksana Elder, Weidong Xiong and Vaithi Arumugaswami (CSMC) for their logistical and technical help, personal assistance and advice. We also appreciate the technical assistance from the Protein Expression Laboratory at NCI-Frederick, the Vector Core at the University of Pennsylvania and the Vector Core (Arumugaswami) laboratory of the Cedars-Sinai Regenerative Medicine Institute. Assistance from the members of several flow cytometry core laboratories was especially appreciated, including Brion Shreffler (University of Pennsylvania), Martha Kirby and Stacie Anderson (NHGRI/NIH) as well as Patricia Lin and Gillian Hultin (Cedars-Sinai Medical Center). We would also like to thank Barrington Burnett (NINDS/NIH) and Mark Burcin (Baylor College of Medine) and Soshana Svendsen (Cedars-Sinai) for advice and critical analysis. We also thank the NIH AIDS Reagent Program, Webster Cavenee (Ludwig Institute for Cancer Research), Steven Goldman (University of Rochester), Hansjörg Hauser (Universität Oldenburg) and Tyler Jacks (MIT) for the generous gifts of plasmids. This research was supported in part by NIH Grant T32-HD043021-04 (to TMP), NIH R01-NS08867 Grant (to JHW), the Intramural Research Program of the NIH/NINDS (to KF) and Cedars-Sinai Medical Center and Board of Governors Regenerative Medicine Institute institutional funding (to CNS, TMP). TMP was also supported by the Diana and Steve Marienhoff Fashion Industries Guild Endowed Fellowship in Pediatric Neuromuscular Diseases.

References

1. Behrstock S, Ebert A, McHugh J, Vosberg S, Moore J, Schneider B, et al. Human neural progenitors deliver glial cell line-derived neurotrophic factor to parkinsonian rodents and aged primates. Gene Therapy. 2006; 13:379–388. [PubMed: 16355116]
2. Cress DE. The need for regulatable vectors for gene therapy for Parkinson's disease. Exp Neurol. 2008; 209:30–33. [PubMed: 17942096]
3. Naidoo J, Young D. Gene regulation systems for gene therapy applications in the central nervous system. Neurol Res Int. 2012; 2012:595410. [PubMed: 22272373]
4. Marmorstein R, Carey M, Ptashne M, Harrison SC. DNA Recognition by GAL4: structure of a protein–DNA complex. Nature. 1992; 356:408–414. [PubMed: 1557122]
5. Wang Y, O'Malley BW Jr, Tsai SY, O'Malley BW. A regulatory system for use in gene transfer. Proc Natl Acad Sci USA. 1994; 91:8180–8184. [PubMed: 8058776]
6. Wang Y, Xu J, Pierson T, O'Malley BW, Tsai SY. Positive and negative regulation of gene expression in eukaryotic cells with an inducible transcriptional regulator. Gene Therapy. 1997; 4:432–441. [PubMed: 9274720]
7. Burcin MM, Schiedner G, Kochanek S, Tsai SY, O'Malley BW. Adenovirus-mediated regulable target gene expression *in vivo*. Proc Natl Acad Sci USA. 1999; 96:355–360. [PubMed: 9892637]
8. Pierson TM, Wang Y, DeMayo FJ, Matzuk MM, Tsai SY, Omalley BW. Regulable expression of inhibin A in wild-type and inhibin alpha null mice. Mol Endocrinol. 2000; 14:1075–1085. [PubMed: 10894156]
9. Nordstrom JL. The antiprogestin-dependent GeneSwitch system for regulated gene therapy. Steroids. 2003; 68:1085–1094. [PubMed: 14668002]
10. Takagi M, Yamakawa H, Watanabe T, Suga T, Junji Y. Inducible expression of long-chain acyl-CoA hydrolase gene in cell cultures. Mol Cell Biochem. 2003; 252:379–385. [PubMed: 14577613]
11. Schilliger KJ, Tsai SY, Taffet GE, Reddy AK, Marian AJ, Entman ML, et al. Regulatable atrial natriuretic peptide gene therapy for hypertension. Proc Natl Acad Sci USA. 2005; 102:13789–13794. [PubMed: 16162668]
12. Emelyanov A, Parinov S. Mifepristone-inducible LexPR system to drive and control gene expression in transgenic zebrafish. Dev Biol. 2008; 320:113–121. [PubMed: 18544450]
13. Maddalena A, Tereshchenko J, Bähr M, Kügler S. Adeno-associated virus-mediated, mifepristone-regulated transgene expression in the brain. Mol Ther Nucleic Acids. 2013; 2:e106. [PubMed: 23860550]

14. Mankodi A, Wheeler TM, Shetty R, Salceies KM, Becher MW, Thornton CA. Progressive myopathy in an inducible mouse model of oculopharyngeal muscular dystrophy. Neurobiol Dis. 2012; 45:539–546. [PubMed: 21964252]
15. Zufferey R, Dull T, Mandel RJ, Bukovsky A, Quiroz D, Naldini L, Trono D. Self-inactivating lentivirus vector for safe and efficient *in vivo* gene delivery. J Virol. 1998; 12:9873–9880. [PubMed: 9811723]
16. Pelletier J, Sonenberg N. Internal initiation of translation of eukaryotic mRNA directed by a sequence derived from poliovirus RNA. Nature. 1988; 334:320–325. [PubMed: 2839775]
17. Lothian C, Lendahl U. An evolutionary conserved region in thr second intron of the human nestin gene directs gene expression to CNS progenitor cells and to early neural crest cells. Eur J Neurosci. 1997; 9:452–462. [PubMed: 9104587]
18. Mullick A, Katzenellenbogen BS. Progesterone receptor synthesis and degradation in MCF-7 human breast cancer cells as studied by dense amino acid incorporation. Evidence for a non-hormone binding receptor precursor. J Biol Chem. 1986; 261:13236–13246. [PubMed: 3759961]
19. Lonard DM, Nawaz Z, Smith CL, O'Malley BW. The 26S proteasome is required for estrogen receptor-alpha and coactivator turnover and for efficient estrogen receptor-alpha transactivation. Mol Cell. 2000; 5:939–948. [PubMed: 10911988]
20. Corish P, Tyler-Smith C. Attenuation of green fluorescent protein half-life in mammalian cells. Protein Eng. 1999; 12:1035–1040. [PubMed: 10611396]
21. Kaster KR, Burgett SG, Rao RN, Ingolia TD. Analysis of a bacterial hygromycin B resistance gene by transcriptional and translational fusions and by DNA sequencing. Nucleic Acids Res. 1983; 11:6895–6911. [PubMed: 6314265]
22. Verkhusha VV, Kuznetsova IM, Stepanenko OV, Zaraisky AG, Shavlovsky MM, Turoverov KK, et al. High stability of *Discosoma* DsRed as compared to *Aequorea* EGFP. Biochemistry. 2003; 42:7879–7884. [PubMed: 12834339]
23. Ebert AD, Barber AE, Heins BM, Svendsen CN. *Ex vivo* delivery of GDNF maintains motor function and prevents neuronal loss in a transgenic mous model of Huntington's disease. Exp Neurol. 2010; 224:155–162. [PubMed: 20227407]
24. Krum JM, Rosenstein JM. Transient coexpression of nestin, GFAP, and vascular endothelial growth factor in mature reactive astroglia following neural grafting or brain wounds. Exp Neurol. 1999; 160:348–360. [PubMed: 10619552]
25. Roll L, Faissner A. Influence of the extracellular matrix on endogenous and transplanted stem cells after brain damage. Front Cell Neurosci. 2014; 8:219. [PubMed: 25191223]
26. Carpenter AE, Jones TR, Lamprecht MR, Clarke C, Kang IH, Friman O, et al. Cell-Profiler: image analysis software for identifying and quantifying cell phenotypes. Genome Biol. 2006; 7:R100. [PubMed: 17076895]
27. Gruh, I.; Martin, U. Transdifferentiation of stem cells: a critical review. In: Martin, U.; Scheper, T., editors. Engineering of Stem Cells. Springer Science & Business Media; Berlin, Germany: 2009. p. 94-96.
28. Schneider CA, Rasband WS, Eliceiri KW. NIH Image to ImageJ: 25 years of image analysis. Nat Methods. 2012; 9:671–675. [PubMed: 22930834]
29. Fillat C, Carrió M, Cascante A, Sangro B. Suicide gene therapy mediated by the Herpes Simplex virus thymidine kinase gene/Ganciclovir system: fifteen years of application. Curr Gene Ther. 2003; 3:13–26. [PubMed: 12553532]
30. Ebert AD, Beres AJ, Barber AE, Svendsen CN. Human neural progenitor cells overexpressing IGF-1 protect dopamine neurons and restore function in a rat model of Parkinson's disease. Exp Neurol. 2008; 209:213–223. [PubMed: 18061591]
31. Kitiyanant N, Kitiyanant Y, Svendsen CN, Thangnipon W. BDNF-, IGF-1 and GDNF-secreting human neural progenitor cells rescue amyloid β-induced toxicity in cultured rat septal neurons. Neurochem Res. 2012; 37:143–152. [PubMed: 21909955]
32. Krakora D, Mulcrone P, Meyer M, Lewis C, Bernau K, Gowing G, et al. Synergistic effects of GDNF and VEGF on lifespan and disease progression in a familial ALS rat model. Mol Ther. 2013; 21:1602–1610. [PubMed: 23712039]

33. Snyder EY, Taylor RM, Wolfe JH. Neural progenitor cell engraftment corrects lysosomal storage throughout the MPS VII mouse brain. Nature. 1995; 374:367–370. [PubMed: 7885477]
34. Svendsen CN, Clarke DJ, Rosser AE, Dunnett SB. Survival and differentiation of rat and human epidermal growth factor-responsive precursor cells following grafting into the lesioned adult central nervous system. Exp Neurol. 1996; 137:376–388. [PubMed: 8635554]
35. Flax JD, Aurora S, Yang C, Simonin C, Wills AM, Billinghurst LL, et al. Engraftable human neural stem cells respond to developmental cues, replace neurons, and express foreign genes. Nat Biotechnol. 1998; 16:1033–1039. [PubMed: 9831031]
36. Gage FH. Mammalian neural stem cells. Science. 2000; 287:1433–1438. [PubMed: 10688783]
37. Tamaki S, Eckert K, He D, Sutton R, Doshe M, Jain G, et al. Engraftment of sorted/expanded human central nervous system stem cells from fetal brain. J Neurosci Res. 2002; 69:976–986. [PubMed: 12205691]
38. McBride JL, Behrstock SP, Chen EY, Jakel RJ, Siegel I, Svendsen CN, et al. Human neural stem cell transplants improve motor function in a rat model of Huntington's disease. Journal Comp Neurol. 2004; 475:211–219.
39. Kelly S, Bliss TM, Shah AK, Sun GH, Ma M, Foo WC, et al. Transplanted human fetal neural stem cells survive, migrate, and differentiate in ischemic rat cerebral cortex. Proc Natl Acad Sci USA. 2004; 101:11839–11844. [PubMed: 15280535]
40. Muller FJ, Snyder EY, Loring JF. Gene therapy: can neural stem cells deliver? Nat Rev Neurosci. 2006; 7:75–84. [PubMed: 16371952]
41. Griffin TA, Anderson HC, Wolfe JH. *Ex vivo* gene therapy using patient iPSC-derived NSCs reverses pathology in the brain of a homologous mouse model. Stem Cell Rep. 2015; 4:835–846.
42. Cummings BJ, Uchida N, Tamaki SJ, Salazar DL, Hooshmand M, Summers R, et al. Human neural stem cells differentiate and promote locomotor recovery in spinal cord-injured mice. Proc Natl Acad Sci USA. 2005; 102:14069–14074. [PubMed: 16172374]
43. Corti O, Sabate O, Horellou P, Colin P, Dumas S, Buchet D, et al. A single adenovirus vector mediates doxycycline-controlled expression of tyrosine hydroxylase in brain grafts of human neural progenitors. Nat Biotechnol. 1999; 17:349–354. [PubMed: 10207882]
44. Takahashi K, Tanabe K, Ohnuki M, Narita M, Ichisaka T, Tomoda K, et al. Induction of pluripotent stem cells from adult human fibroblasts by defined factors. Cell. 2007; 131:861–872. [PubMed: 18035408]
45. Yu J, Vodyanik MA, Smuga-Otto K, Antosiewicz-Bourget J, Frane JL, Tian S, et al. Induced pluripotent stem cell lines derived from human somatic cells. Science. 2007; 318:1917–1920. [PubMed: 18029452]
46. Sareen D, Gowing G, Sahabian A, Staggenborg K, Paradis R, Avalos P, et al. Human induced pluripotent stem cells are a novel source of neural progenitor cells (iNPCs) that migrate and integrate in the rodent spinal cord. J Comp Neurol. 2014; 522:2707–2728. [PubMed: 24610630]
47. Miyoshi H, Blomer U, Takahashi M, Gage FH, Verma IM. Development of a self-inactivating lentivirus vector. J Virol. 1998; 72:8150–8157. [PubMed: 9733856]
48. Heuer GG, Skorupa AF, Prasad Alur RK, Jiang K, Wolfe JH. Accumulation of abnormal amounts of glycosaminoglycans in murine mucopolysaccharidosis type VII neural progenitor cells does not alter the growth rate or efficiency of differentiation into neurons. Mol Cell Neurosci. 2001; 17:167–178. [PubMed: 11161477]
49. Boockvar JA, Kapitonov D, Kapoor G, Schouten J, Counelis GJ, Bogler O, et al. Constitutive EGFR signaling confers a motile phenotype to neural stem cells. Mol Cell Neurosci. 2003; 24:1116–1130. [PubMed: 14697673]
50. Hahne F, LeMeur N, Brinkman RR, Ellis B, Haaland P, Sarkar D, et al. flowCore: a Bioconductor package for high throughput flow cytometry. BMC Bioinform. 2009; 10:106.
51. Gentleman RC, Carey VJ, Bates DM, Bolstad B, Dettling M, Dudoit S, et al. Bioconductor: open software development for computational biology and bioinformatics. Genome Biol. 2004; 5:R80. [PubMed: 15461798]
52. RStudio. RStudio: Integrated development environment for R (Version 0.98.501). Computer software; Boston, MA, USA: 2013. Available at: http://www.rstudio.org (accessed 11 December 2014)

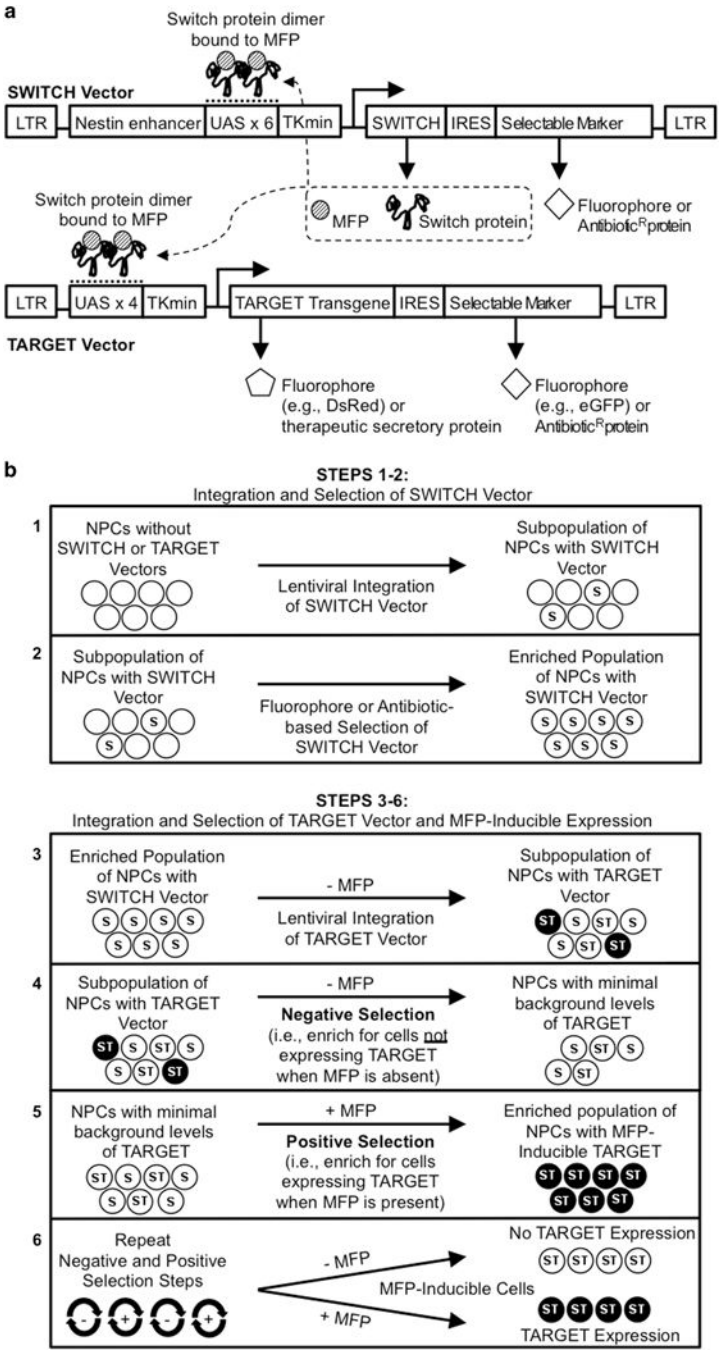

Figure 1.

SWITCH and TARGET vectors used for MFP-inducible expression and strategy for generating MFP-inducible cells *in vitro*. (**a**) Lentiviral SWITCH vectors express the SWITCH gene linked via a poliovirus IRES to a selectable-marker gene (encoding a fluorophore or antibiotic-resistance protein) from an auto-inducible promoter consisting of the second intron enhancer of the rat nestin gene, GAL4 autoregulatory elements and a minimal herpesvirus thymidine kinase promoter. Lentiviral TARGET vectors are also expressed from an MFP-inducible promoter upstream of a TARGET transgene and a

selectable-marker gene (e.g., a fluorophore or antibiotic-resistance gene) for both negative and positive selection. Gene expression is induced at both loci with exposure to MFP, resulting in the activation and dimerization of the SWITCH protein, which then binds to the UAS sequences in their respective promoters. (**b**) Strategy for integration and selection of the SWITCH vectors in neural progenitor cells (STEPS 1 and 2). Strategy for integration and negative and positive selection of NPCs with MFP-inducible expression (STEPS 3–6). LTR, long terminal repeat; S, cells integrated with SWITCH vector; T, cells integrated with TARGET vector; TKmin, minimal thymidine kinase promoter; white circle, no expression of Target transgene(s); black circle, expression of Target transgene(s).

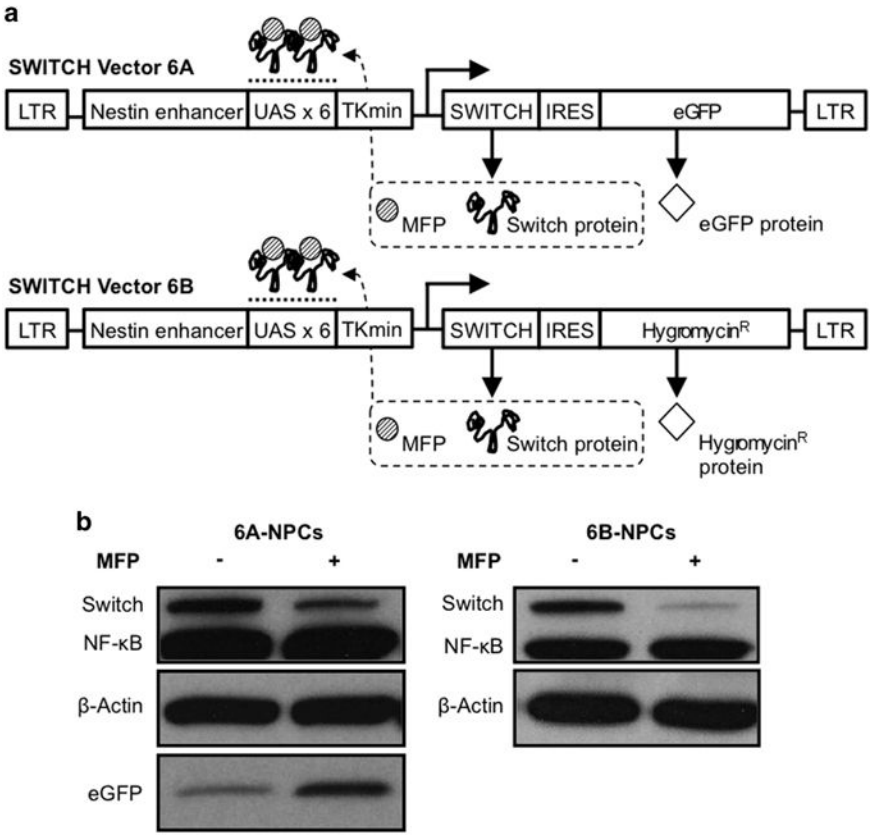

Figure 2.

SWITCH Vectors 6A and 6B and western blot analysis of transgene protein levels following MFP exposure. (**a**) SWITCH vectors use a fluorophore (vector 6A) or antibiotic-resistance gene (vector 6B) for selection-based enrichment. (**b**) Western blot analysis of mNPC lysates from 6A- and 6B-NPCs. 6A-NPCs demonstrated an increase in eGFP protein expression following MFP exposure. Both 6A- and 6B-NPC cell lysates demonstrated the expression of SWITCH protein that paradoxically decreased with MFP treatment following MFP exposure. This decrease was a result of activation-dependent degradation. SWITCH protein was detected using an anti-nuclear factor-κB (NF-κB) antibody, an anti-β-actin antibody was used to show equivalent loading of protein lysates. LTR, long terminal repeat.

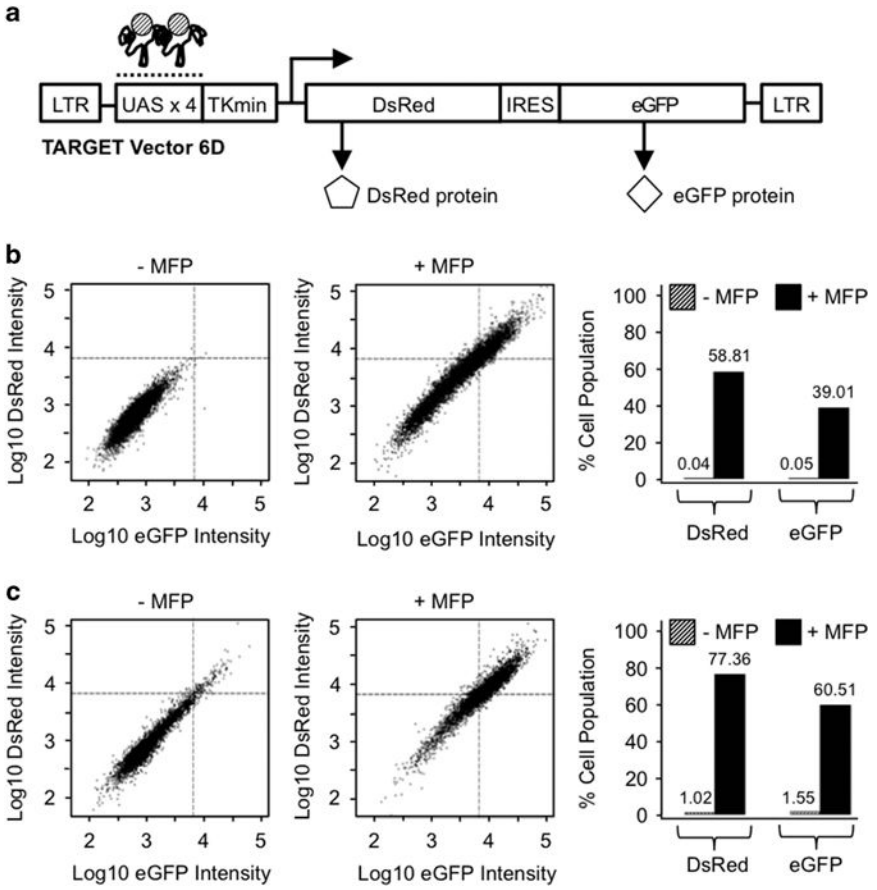

Figure 3.

TARGET vector 6D and stringent versus relaxed selection protocols. (**a**) Inducible expression of two target genes, monomeric DsRed and eGFP from vector 6D. This vector was used to characterize the MFP-inducible expression of this system both *in vitro* and *in vivo*. (**b** and **c**) Fluorescence intensities (arbitrary units) of both DsRed and eGFP were evaluated by flow cytometry using 10 000 cells as input (before gating). Positive and negative selection steps were performed with FACS. Cell populations were obtained after a final sort using either a (**b**) negative selection (stringent) protocol or (**c**) positive selection (relaxed) protocol. These populations were evaluated for fluorescence intensities in the absence (−) or presence (+) of MFP. Dotted lines in scatter plots of DsRed/eGFP intensities represent our definitive threshold value (log10 = 3.8) for positive expression of these fluorophores. Bar graphs represent the percent of the cell population that was above this threshold value (log10 = 3.8) for both eGFP and DsRed with either stringent (**b**) or relaxed (**c**) protocols. LTR, long terminal repeat.

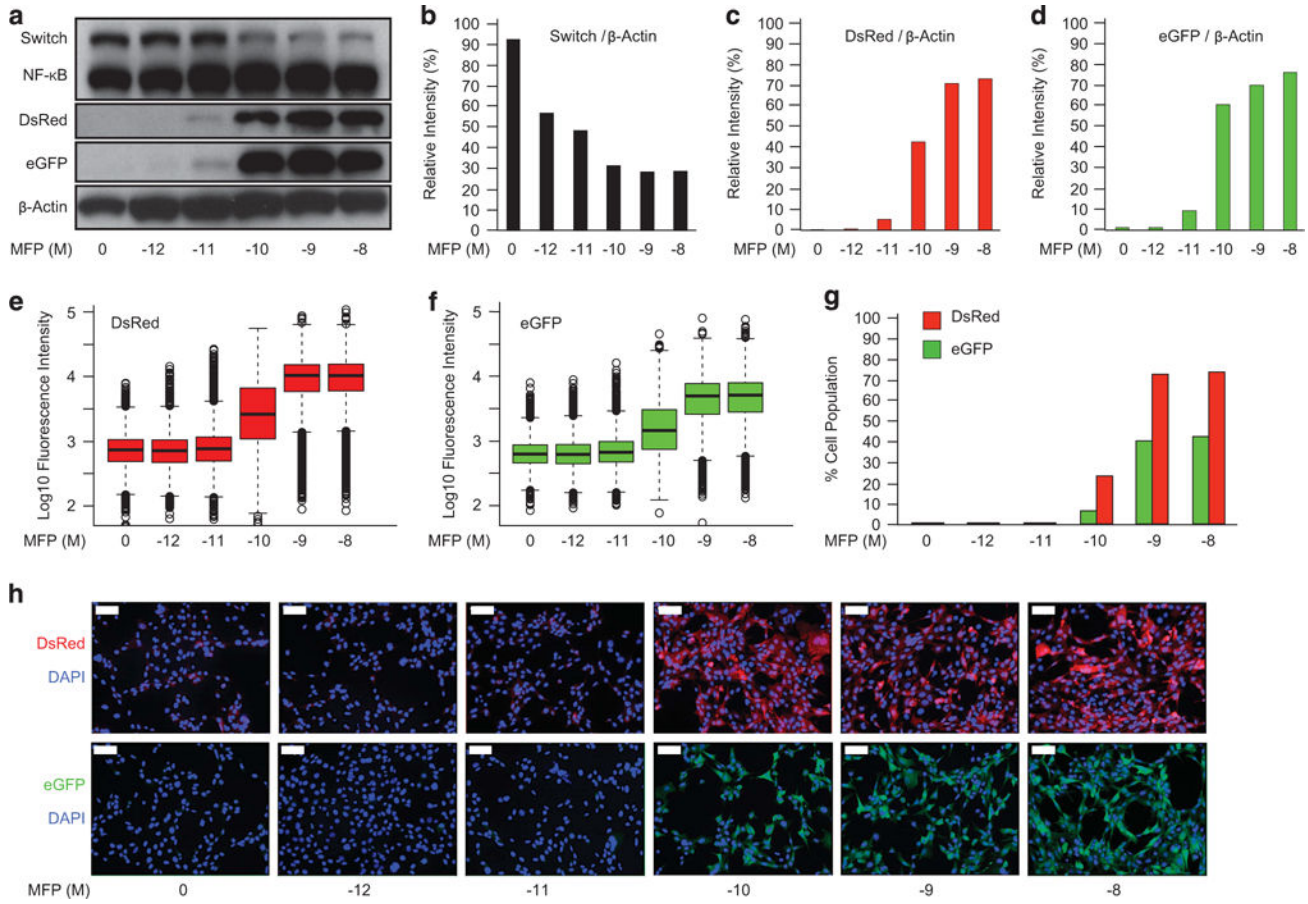

Figure 4.

Dose-dependent expression of TARGET genes following MFP exposure. 6B6D-NPCs were exposed to MFP (10^{-12}–10^{-8} M) for 2–4 days, and cells or cell lysates were used to analyze the expression of the DsRed and eGFP target genes. (**a**) Western blot analysis demonstrated a dose-dependent increase in DsRed and eGFP protein levels associated with a dose-dependent decrease in SWITCH protein levels. (**b–d**) Bar graphs representing ImageJ software analyses of relative intensities of (**b**) SWITCH, (**c**) DsRed and (**d**) eGFP, all normalized to β-actin. (**e** and **f**) Box-and-whisker plots of fluorescence intensities (arbitrary units) of target genes measured by flow cytometry using 10 000 cells as input (before gating). A dose-dependent increase in both DsRed (**e**) and eGFP (**f**) was observed following MFP exposure. (**g**) Bar graphs represent the percent of the cell population that was above our threshold value (log10 = 3.8) for both eGFP and DsRed. (**h**) Immunocytochemistry and epifluorescent imaging analysis of target gene expression following MFP exposure. Images represent antibody-amplified DsRed expression (red) and the nuclear counterstain DAPI (blue), or antibody-amplified eGFP expression (green) and the nuclear counterstain DAPI (blue). Scale bars = 50 μm. NF-κB, nuclear factor-κB.

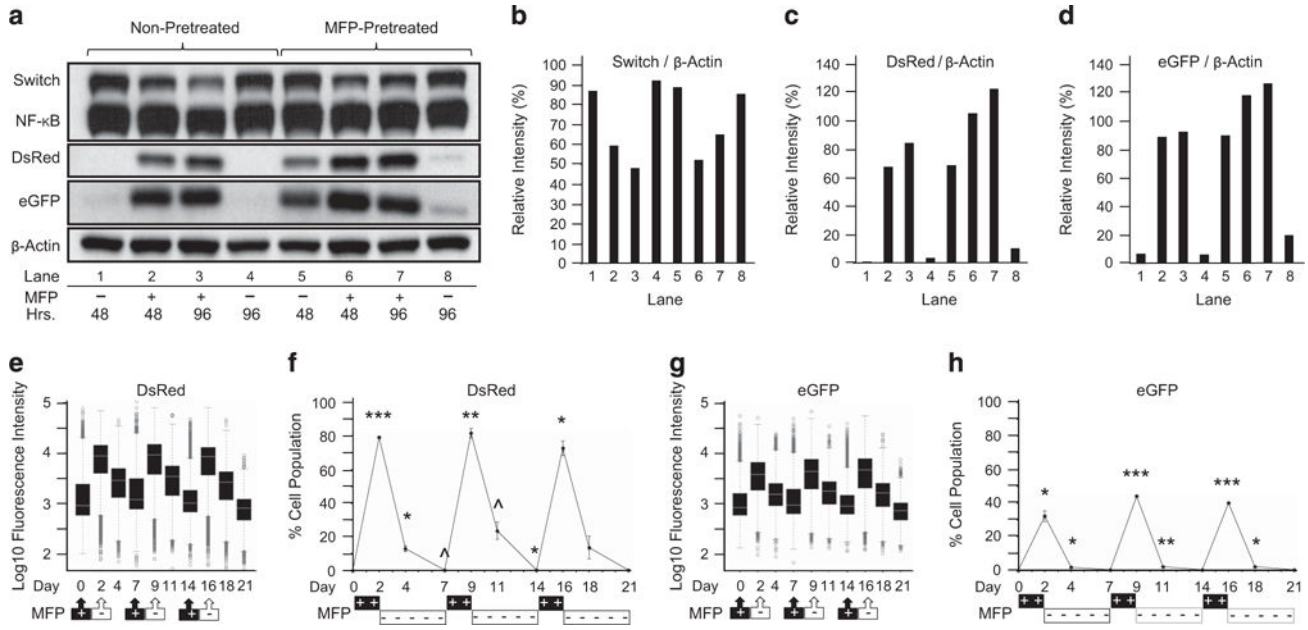

Figure 5.

Target gene expression in MFP-inducible 6B6D-NPCs can be repeatedly activated and deactivated. (a) Western blot analysis of MFP-inducible NPCs after exposure or withdrawal of MFP. 6B6D-NPCs were either pretreated (right) or not pretreated (left) with MFP for ⩾ 96 h. 6B6D-NPCs were then exposed to media with (+) or without (−) MFP and cell lysates were collected after 48 and 96 h. (**b–d**) Bar graphs representing ImageJ software analyses of relative intensities of (**b**) Switch, (**c**) DsRed and (**d**) eGFP, all relative to β-actin. (**e–h**) Flow cytometry analysis of a 21-day *in vitro* time series when target gene expression was activated and deactivated over three cycles (2 days of MFP treatment followed by 5 days of MFP withdrawal). MFP was added to cells (days 0, 7 and 14), or removed from cells (days 2, 9 and 16) after they were collected for flow cytometry analysis. (**e** and **g**) Box-and-whisker plots of fluorescence intensities (arbitrary units) of (**e**) DsRed and (**g**) eGFP measured by flow cytometry using 10 000 cells as input (before gating). (**f** and **h**) Bar graphs representing the percent of the cell population that was above our threshold value of positive expression (log 10 = 3.8) for both (**f**) DsRed and (**h**) eGFP during this 21-day *in vitro* activation and deactivation series. This time series was repeated, for a total of three experimental replicates. Error bars represent mean fluorescence ± s.d., from three independent experiments. Statistics shown are from Welch's *t*-tests between each available timepoint and the day 0 samples. ^P<0.05, *P<0.01, **P<0.001 and ***P<0.0001. NF-κB, nuclear factor-κB.

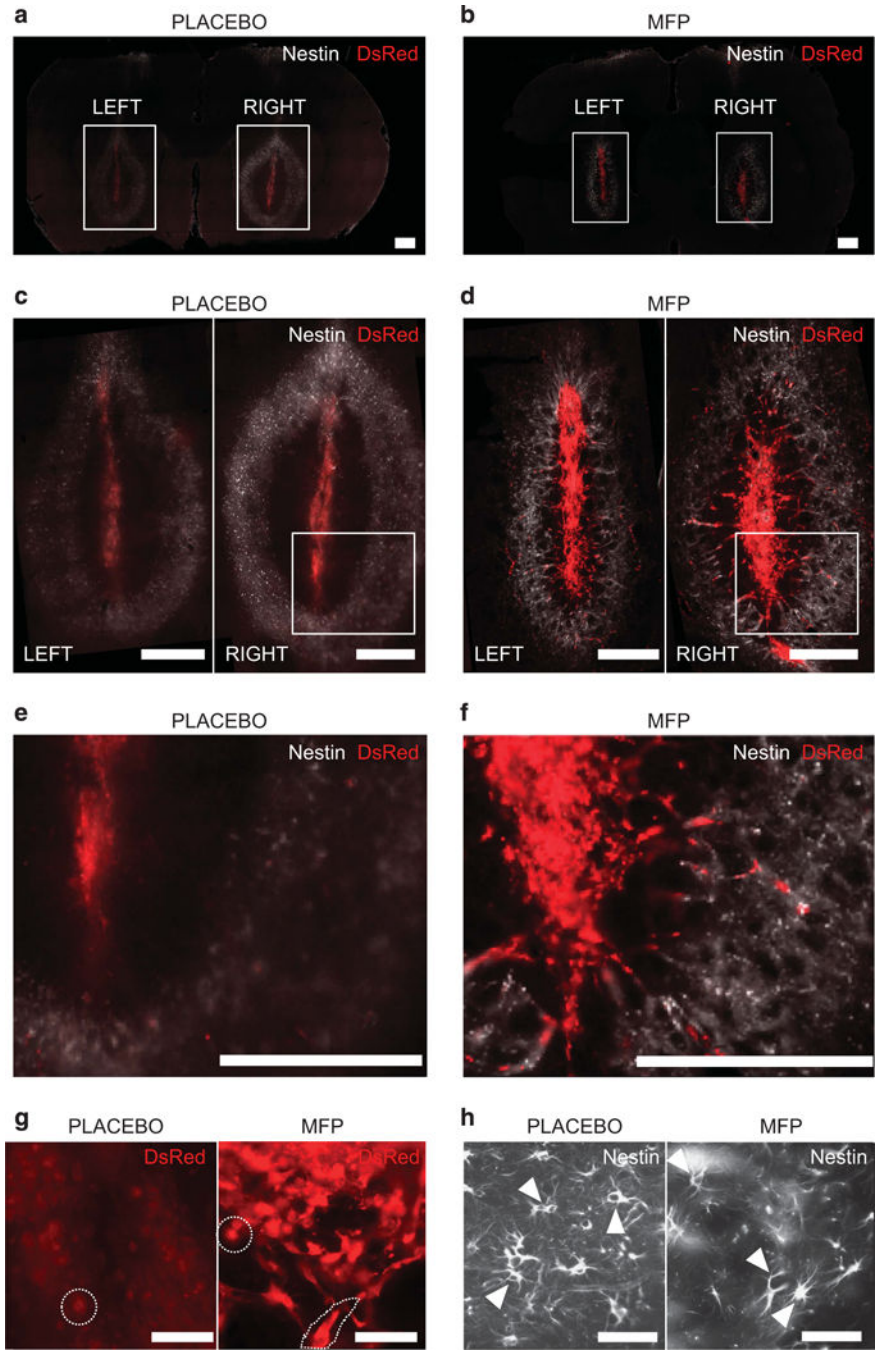

Figure 6.

Transplantation of MFP-inducible 6B6D-NPCs into the rat striatum and *in vivo* activation or inactivation of target gene expression with exposure to MFP or placebo. Rats were implanted subcutaneously with 21-day timed-release (**a**, **c** and **e**) placebo, or (**b**, **d** and **f**) MFP pellets. Three days later, MFP-inducible 6B6D-NPCs that had been pretreated *in vitro* with 10^{-8} M MFP for >1 week before surgery were injected into the right striatum, whereas non-treated cells were injected into the left striatum. (**a** and **b**) Transplanted cell grafts were localized in tissue sections using an anti-nestin antibody (white), which detected a ‘ring’ of

endogenous nestin-positive reactive cells that had surrounded the graft. Expression of the TARGET gene, DsRed, was evaluated using an anti-DsRed antibody (red). (**c** and **d**) Visual evaluation of grafts demonstrated no noticeable difference between the right and left hemispheres (i.e., no effect from *in vitro* pretreatment), but showed a noticeable effect of *in vivo* MFP exposure. (**e** and **f**) Close-up view of boxed regions shown in (**c** and **d**). (**g**) High-resolution images of red fluorescent cells in rats treated with placebo (left) displayed a rounded morphology (see dotted lines) and were centrally located to the graft, suggesting most fluorescence was the result of autofluorescence from dead cells. MFP-treated rats (right) displayed red fluorescence in both rounded and spindle-shaped cells (see dotted lines), the latter being indicative of healthy cells expressing DsRed. (**h**) High-resolution images of endogenous nestin-positive reactive cells (arrow heads) around the graft in placebo (left) and MFP-treated (right) rats. Scale bars: (**a**–**f**) 500 μm; (**g** and **h**) 50 μm.

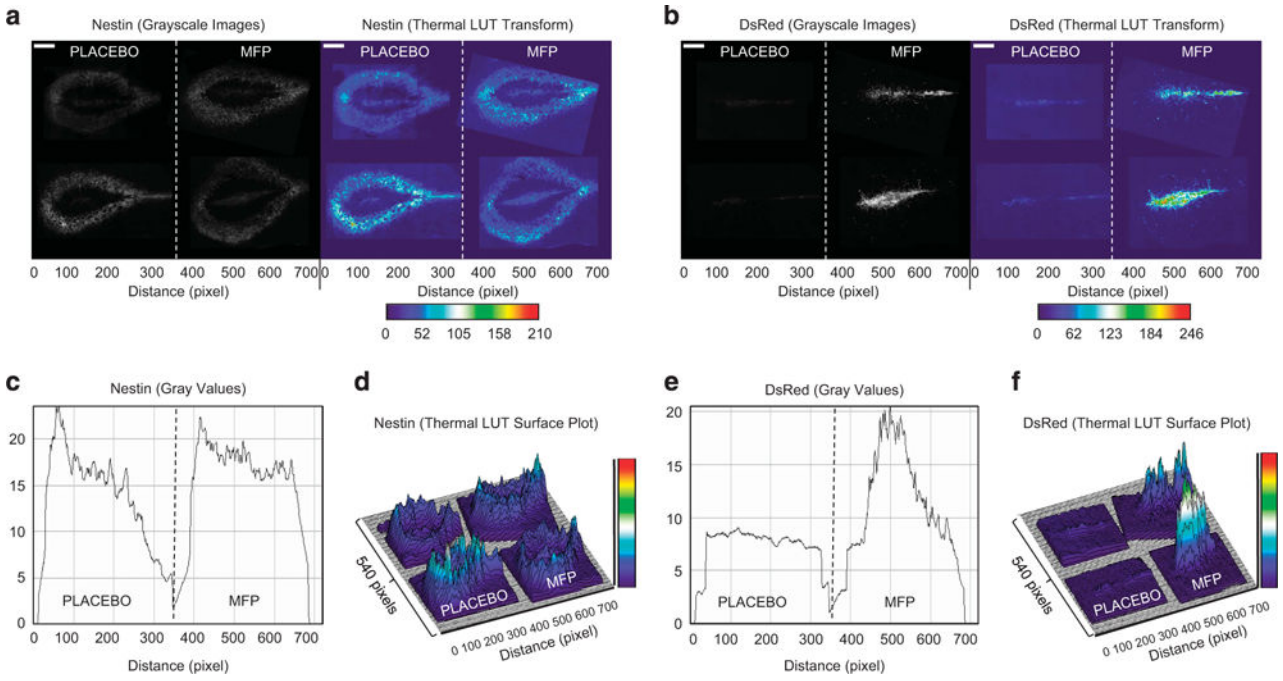

Figure 7.

MFP-inducible cell grafts across multiple rats and image analysis of fluorescence intensities. Placebo- versus MFP-treated rats were compared for transgene expression ($N = 2$). Brain grafts from each rat were compiled into a single image, and pixel intensities across all four grafts were evaluated for both nestin and DsRed reactivity using ImageJ software. (**a**) Compiled grayscale images of nestin-positive 'ring' of reactive cells and nestin-positive transplanted 6B6D-NPCs in rats given placebo (left) or MFP (right), and thermal Math Lookup Table (LUT) transformation of grayscale image. (**b**) Compiled grayscale images of DsRed-positive transplant in rats given placebo (left) or MFP (right), and thermal LUT transformation of grayscale image. (**c**) Plot of gray values across merged grayscale image in (**a**). (**d**) Surface plot of thermal LUT transform image in (**a**). (**e**) Plot of gray values across merged grayscale image in (**b**). (**f**) Surface plot of thermal LUT transform image in (**b**).

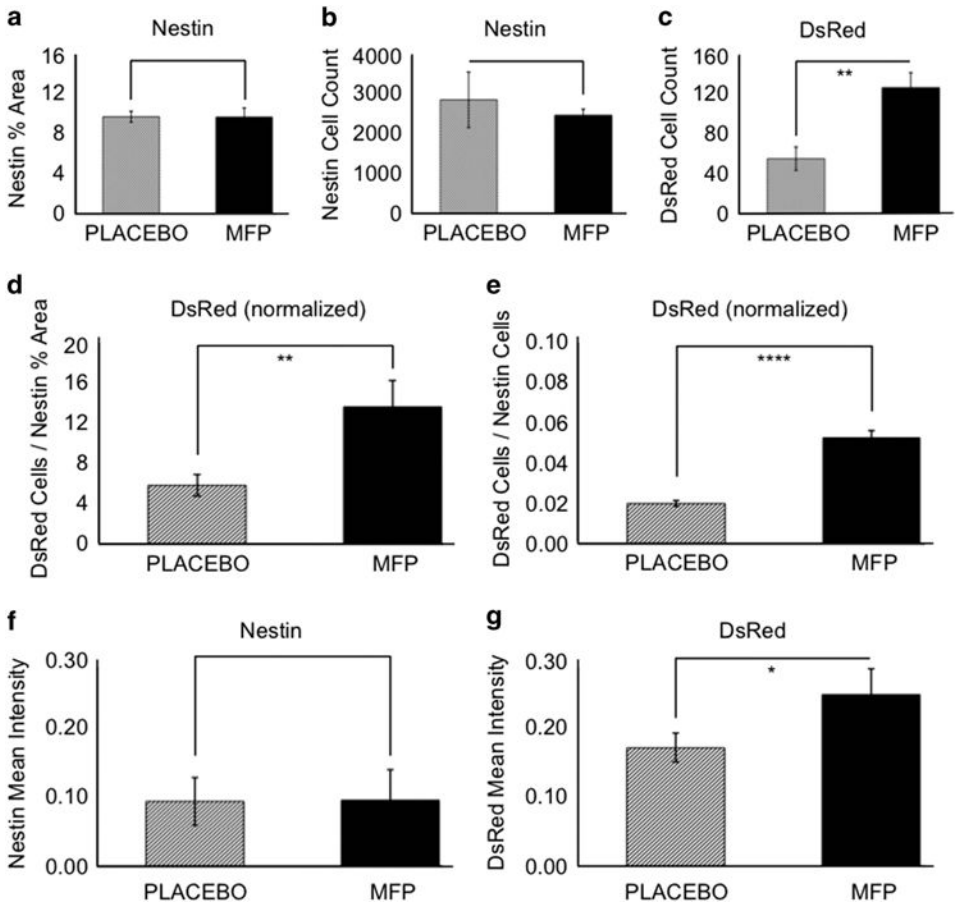

Figure 8.

Statistical analysis of transplanted MFP-inducible 6B6D-NPCs adjacent to the graft site in multiple rats. Immunoreactivity of 6B6D-NPCs migrating through regions near the graft site was compared in placebo- versus MFP-treated rats ($N = 3$). Brain sections were identified that contained a dense cluster of endogenous nestin-positive reactive cells that were adjacent to, but did not include, the core of the graft site to quantitate DsRed immunoreactivity without the confounding effects of autofluorescence in the graft core. To verify that similar sections were chosen for statistical analysis, images were evaluated (and normalized) for nestin immunoreactivity by both cell counts and image intensity, and DsRed immunoreactivity of each section was also quantitated. (**a–g**) CellProfiler software image and cell quanification analyses of immunoreactive intensities for the (**a**) mean percent of each image area with nestin immunoreactivity in each group ($P = 0.9586$), (**b**) the mean number of nestin objects (cells) that were counted in each group ($P = 0.4023$), (**c**) the mean number of DsRed objects (cells) that were counted in each group, (**d**) the mean number of DsRed cells, normalized to the percent image area that had nestin reactivity (data from c/a) in each group, (**e**) the mean number of DsRed cells, normalized to the number of nestin objects (data from c/b) in each group, (**f**) the mean fluorescence intensity of the nestin images in each group and (**g**) the mean fluorescence intensities of the DsRed objects (cells) in each group. Error bars represent mean ± s.d. ($N = 3$). Parametric *t*-tests comparing rats

given placebo versus MFP are shown for each analysis. *P<0.05, **P<0.01 and ****P<0.0001.